external): $\delta = -5.8, -10.5, -16.0$ (2:6:2); $^{199}Hg\{^1H\}$ NMR (89.6 MHz, acetone, 25 °C, external 0.5 M PhHgCl in [D$_6$]DMSO: chemical shift $\delta = -1187$[22] upfield from neat Me_2Hg): $\delta = -622$; negative-ion FAB-MS: m/z (%): 2505 (100) $[\mathbf{1}\cdot I]^-$, 2640 (45) $Li[\mathbf{1}\cdot I_2]^-$.

Received: March 1, 2001 [Z16708]

[1] M. F. Hawthorne, Z. Zheng, *Acc. Chem. Res.* **1997**, *30*, 267 – 276.

[2] Examples of multidentate Lewis acids: a) M. Tsunoda, F. P. Gabbaï, *J. Am. Chem. Soc.* **2000**, *122*, 8335 – 8336; b) M. Tschinkl, A. Schier, J. Riede, F. P. Gabbaï, *Angew. Chem.* **1999**, *111*, 3769 – 3771; *Angew. Chem. Int. Ed.* **1999**, *38*, 3547 – 3549; c) T. Ooi, T. Miura, K. Maruoka, *Angew. Chem.* **1998**, *110*, 2524 – 2526; *Angew. Chem. Int. Ed.* **1998**, *37*, 2347 – 2349; d) J. D. Wuest, *Acc. Chem. Res.* **1999**, *32*, 81 – 89; e) R. Altmann, K. Jurkschat, M. Schürmann, *Organometallics* **1998**, *17*, 5858 – 5866; f) M. Tschinkl, A. Schier, J. Riede, F. P. Gabbä, *Inorg. Chem.* **1997**, *36*, 5706 – 5711; g) F. P. Schmidtchen, M. Berger, *Chem. Rev.* **1997**, *97*, 1609 – 1646; h) P. D. Beer, D. K. Smith in *Progress in Inorganic Chemistry*, *Vol. 46* (Ed.: K. D. Karlin), Wiley, New York, **1997**, pp. 1 – 97.

[3] H. Lee, M. Diaz, C. B. Knobler, M. F. Hawthorne, *Angew. Chem.* **2000**, *112*, 792 – 794; *Angew. Chem. Int. Ed.* **2000**, *39*, 776 – 778.

[4] a) I. H. A. Badr, R. D. Johnson, M. Diaz, M. F. Hawthorne, L. G. Bachas, *Anal. Chem.* **2000**, *72*, 4249 – 4254; b) I. H. A. Badr, M. Diaz, M. F. Hawthorne, L. G. Bachas, *Anal. Chem.* **1999**, *71*, 1371 – 1377.

[5] H. Lee, M. Diaz, M. F. Hawthorne, *Tetrahedron Lett.* **1999**, *40*, 7651 – 7655.

[6] J. Li, C. F. Logan, M. Jones, Jr., *Inorg. Chem.* **1991**, *30*, 4866 – 4868.

[7] Z. Zheng, C. B. Knobler, M. D. Mortimer, G. Kong, M. F. Hawthorne, *Inorg. Chem.* **1996**, *35*, 1235 – 1243.

[8] a) H. Lee, C. B. Knobler, M. F. Hawthorne, *Chem. Commun.* **2000**, 2485 – 2486; b) G. Harakas, T. Vu, C. B. Knobler, M. F. Hawthorne, *J. Am. Chem. Soc.* **1998**, *120*, 6405 – 6406.

[9] P. C. Andrews, C. L. Raston, *J. Organomet. Chem.* **2000**, *600*, 174 – 185.

[10] a) M. J. Hardie, C. L. Raston, *Eur. J. Inorg. Chem.* **1999**, 195 – 200; b) P. D. Godfrey, W. J. Grigsby, P. J. Nichols, C. L. Raston, *J. Am. Chem. Soc.* **1997**, *119*, 9283 – 9284.

[11] R. N. Grimes, *Carboranes*, Academic Press, New York, **1970**, p. 66.

[12] Crystallographic data collection for $[Li_2\{(CH_3)_2CO\}_6][\mathbf{1}_2\cdot I]\supset 4H_2O$: $C_{13}H_{34}B_{20}Hg_2I_5LiO_5$, $M_r = 1529.22$, crystal dimensions $= 0.15 \times 0.15 \times 0.25$ mm^3, monoclinic, space group $C2/m$, $a = 31.26(1)$, $b = 22.14(1)$, $c = 7.068(3)$ Å, $\beta = 94.463(9)°$, $V = 4876(4)$ Å^3, $Z = 2$, $\rho_{calcd} = 2.083$ mg cm^{-3}, $T = 100(2)$ K, absorption coefficient $\mu = 9.476$ mm^{-1}. Data were collected on a Bruker SMART CCD diffractometer, using $Mo_{K\alpha}$ radiation ($\lambda = 0.71073$ Å). Unit cell parameters were determined from a least-squares fit of 916 accurately centered reflections ($4.33° < 2\theta < 55.80°$). A total of 6001 unique reflections were measured, of which 3832 reflections were considered observed with $I > 2\sigma(I)$. All reflections were used for structure analysis. The intensity data were corrected for Lorentz and polarization effects, absorption, and secondary extinction. Atoms were located by use of heavy atom methods. With the exception of Li, all non-hydrogen atoms were refined with anisotropic parameters. With the exception of H of water (not located), all H were included in structure factor calculations but parameters were not refined. The H atoms were assigned isotropic displacement values based approximately on the value for the attached atom. The final discrepancy index was $R = 0.055$, $R_w = 0.133$ ($w = 1/\sigma^2(|F_0|)$) for 3832 independent reflections with $I > 2\sigma(I)$. The largest peak maximum and minimum on a final difference electron density map were 2.724 and -3.020 e Å^{-3}, both near Hg. Data were processed by using the Bruker SMART 1000 software package. Crystallographic data (excluding structure factors) for the structure reported in this paper have been deposited with the Cambridge Crystallographic Data Centre as supplementary publication no. CCDC-158870. Copies of the data can be obtained free of charge on application to CCDC, 12 Union Road, Cambridge CB2 1EZ, UK (fax: (+44) 1223-336-033; e-mail: deposit@ccdc.cam.ac.uk).

[13] A. J. Canty, G. B. Deacon, *Inorg. Chim. Acta* **1980**, *45*, L225-L227.

[14] L. Pauling, *The Nature of the Chemical Bond*, 3rd ed., Cornell University Press, Ithaca, **1960**, p. 260.

[15] X. Yang, C. B. Knobler, M. F. Hawthorne, *J. Am. Chem. Soc.* **1992**, *114*, 380 – 382.

[16] V. B. Shur, I. A. Tikhonova, A. I. Yanovsky, Y. T. Struchkov, P. V. Petrovskii, S. Y. Panov, G. G. Furin, M. E. Vol'pin, *Dokl. Akad. Nauk SSSR* **1991**, *321*, 1002 – 1004.

[17] A. Bondi, *J. Phys. Chem.* **1964**, *68*, 441 – 451.

[18] Angle B9-I9-I9′-B9′ = 180°. a) V. R. Pedireddi, D. S. Reddy, B. S. Goud, D. C. Craig, A. D. Rae, G. R. Desiraju, *J. Chem. Soc. Perkin Trans. 2* **1994**, 2354 – 2360; b) G. R. Desiraju, R. Parthasarathy, *J. Am. Chem. Soc.* **1989**, *111*, 8725 – 8726.

[19] Distances between iodide ··· iodide, and H ··· H in Figure 3 were calculated by using atomic van der Waals radii.[14]

[20] O. M. Yaghi, H. Li, C. Davis, D. Richardson, T. L. Groy. *Acc. Chem. Res.* **1998**, *31*, 474 – 484.

[21] a) J. S. Seo, D. Whang, H. Lee, S. I. Jun, J. Oh, Y. J. Jeon, K. Kim, *Nature* **2000**, *404*, 982 – 986; b) A. Heckel, D. Seebach, *Angew. Chem.* **2000**, *112*, 165 – 167; *Angew. Chem. Int. Ed.* **2000**, *39*, 163 – 165; c) T. Sawaki, T. Dewa, Y. Aoyama, *J. Am. Chem. Soc.* **1998**, *120*, 8539 – 8540.

[22] M. A. Sens, N. K. Wilson, P. D. Ellis, J. D. Odom, *J. Magn. Reson.* **1975**, *19*, 323 – 336.

Optically Tuning the Rate of Stoichiometry Changes: Surface-Controlled Oxygen Incorporation into Oxides under UV Irradiation

Rotraut Merkle, Roger A. De Souza, and Joachim Maier*

Stoichiometry changes are fundamental to all solid-state chemical reactions and thus one of the most central processes in solid-state chemistry. Moreover, the relevant stoichiometry determines whether an ionic material is ionically or electronically conducting, whether it is an n- or p-type electronic conductor, and may even determine whether or not it is superconducting. The kinetics of in- and excorporation reactions are also directly involved in the functioning of electroceramic devices, such as permeation membranes, electrodes in fuel cells, and chemical sensors.[1–4] The stoichiometry change process consists of surface reaction steps in series with a bulk diffusion step, of which the former become increasingly important at lower temperatures.

In this Communication, we present results on the use of UV light to tune the rate of oxygen incorporation into the bulk of a model mixed conductor, iron-doped $SrTiO_3$, by altering the rate of the surface reaction under conditions where the surface reaction determines the overall kinetics of the stoichiometry change. While the effects of illumination on the surface composition (see, for example, refs. [5, 6]) and on the catalytic activity of wide-bandgap semiconductors have drawn much attention, for example with regard to the photolysis of water, the selective oxidation of hydrocarbons, and the removal of organic pollutants from air or water,[7–10] the effect of irradiation on the kinetics of bulk stoichiometry changes (in the surface-controlled regime) has, to the best of our knowledge, not yet been reported.

[*] Prof. Dr. J. Maier, Dr. R. Merkle, Dr. R. A. De Souza
Max-Planck-Institut für Festkörperforschung
Heisenbergstrasse 1, 70569 Stuttgart (Germany)
Fax: (+49) 711-689-1722
E-mail: weiglein@chemix.mpi-stuttgart.mpg.de

  1433-7851/01/4011-2126 $ 17.50+.50/0

The stoichiometry relaxation experiments were performed on single crystalline iron-doped $SrTiO_3$, a material for which the defect chemical parameters and transport properties of the bulk are well known.[11–14] In $SrTiO_3$, Fe substitutes onto the Ti site and is present as both Fe^{3+} and Fe^{4+}; the ratio of the valence states depends on temperature and oxygen partial pressure. Fe^{3+} ions on Ti^{4+} sites are negatively charged defects and are mainly compensated by oxygen vacancies, whose concentration is large compared with the concentration of electron holes, the majority electronic carrier. The concentrations of all relevant defects, which were calculated for an oxygen partial pressure $P_{O_2} = 0.1$ bar from parameters given in ref. [11], are shown in Figure 1.

Oxygen incorporation into $SrTiO_3$ occurs by oxygen molecules annihilating oxygen vacancies to produce electron holes. Under a local electronic equilibrium, the increased concentration of holes gives rise to an increase in the concentration of Fe^{4+} (at the expense of Fe^{3+}). Thus, Fe^{4+} ions provide a sensitive measure of the oxygen stoichiometry of the sample. Oxygen in- or excorporation due to changes in P_{O_2} can consequently be followed in situ by spectroscopically monitoring the visible absorption band of Fe^{4+} centered at 590 nm (absorption of Fe^{3+} coincides with $SrTiO_3$ bandgap absorption). For the irradiation experiments, we examined the effect of photon energies above and below the bandgap energy.

Generally, surface and diffusion kinetics are both important with regard to the stoichiometry relaxation of a $SrTiO_3$ sample after a sudden P_{O_2} change. Within the range of conditions of this study, defined by the sample dimensions, bare polished surfaces, temperatures, and oxygen partial pressures, the oxygen transport was essentially controlled by the surface kinetics,[15, 16] that is the chemical diffusion of oxygen in the bulk is much faster than the surface reaction rate and hence the vacancy concentration is almost constant across the sample. The oxygen vacancy concentration, $[\square]$, which is linearly related to the absorbance A of the Fe^{4+} band,[8] then follows an exponential rate law, which depends only on an effective rate constant, $\bar{k}^{\delta}$, and the sample thickness, $2L$.

Data obtained under UV irradiation could also be described by Equation (1), even though the two sides of the sample were not identical. We have to replace $\bar{k}^{\delta}$ therefore with an effective quantity $\langle \bar{k}^{\delta}_{UV} \rangle$. It was found from finite difference calculations that $\langle \bar{k}^{\delta}_{UV} \rangle$ was, to a good approximation, the arithmetic mean of $\bar{k}^{\delta}_{UV}$ of the irradiated surface and of $\bar{k}^{\delta}$ of the unirradiated back surface (that is, the error introduced was negligible for all experiments performed).

$$\frac{[\square]_t - [\square]_{t=\infty}}{[\square]_{t=0} - [\square]_{t=\infty}} = \frac{A_t - A_{t=\infty}}{A_{t=0} - A_{t=\infty}} = 1 - \exp\left(\frac{-k^{\delta} t}{L}\right) \quad (1)$$

First, let us briefly consider the stoichiometric relaxation kinetics without irradiation. These $\bar{k}^{\delta}$ values are plotted versus the final oxygen partial pressure in Figure 2a. It is seen that

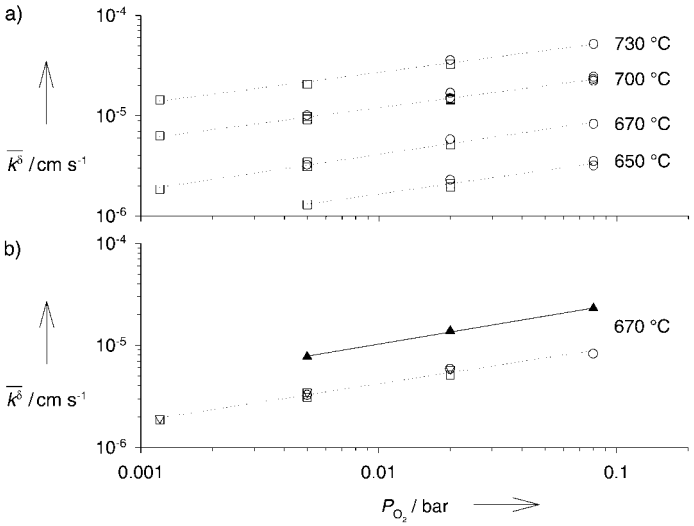

Figure 2. Effective rate constants as a function of final P_{O_2}: a) $\bar{k}^{\delta}$, for oxygen in- (circles) and excorporation (squares); b) $\bar{k}^{\delta}$ for oxygen in- (circles) and excorporation (squares), and $\bar{k}^{\delta}_{UV}$ for oxygen in- (solid triangles) and excorporation (open triangles).

the $\bar{k}^{\delta}$ values obtained for partial pressure jumps to the same final P_{O_2}, either from lower or higher P_{O_2} values, are identical within experimental error. The P_{O_2} dependence of $\bar{k}^{\delta}$, determined from linear regression analysis, is $\bar{k}^{\delta} \propto P_{O_2}^{0.33\pm0.02}$ at all the temperatures examined. The fact that the exponent is the same for all (fairly high) temperatures examined is evidence that the fraction of surface sites occupied by adsorbed species is very small. The Arrhenius plots of $\bar{k}^{\delta}$ (Figure 3) yield an effective activation energy of 274 ± 2 kJ mol^{-1}, which is independent of P_{O_2}.

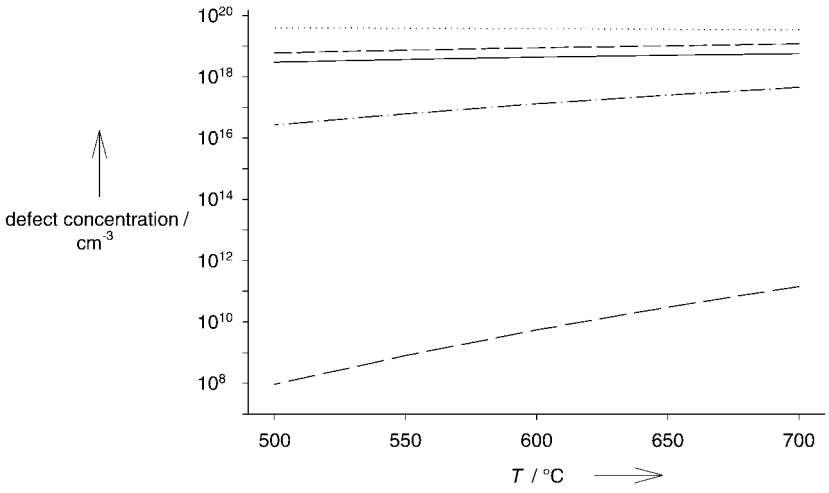

Figure 1. Defect concentrations in Fe-doped $SrTiO_3$ (Fe content $= 4.6 \times 10^{19}$ cm^{-3}) at $P_{O_2} = 0.1$ bar calculated from known defect chemical parameters.[11] Dotted: Fe^{4+}, short dash: Fe^{3+}, solid: oxygen vacancies, dot-dash: electron holes, long dash: conduction electrons.

We first examined the effect of UV irradiation on an equilibrated sample (no P_{O_2} jump). After an irradiation period of 1 h, the absorbance had increased slightly, although the change was small compared to the absorbance changes due to the P_{O_2} jumps. For conditions other than those considered here, the effect can be significant. A detailed analysis of this will be given elsewhere. The relaxation after the irradiation period took place on the same time scale as the stoichiometry relaxation after a jump in P_{O_2}.

For UV irradiation during stoichiometry change experiments, irradiation had no measurable effect for jumps from higher to lower P_{O_2}

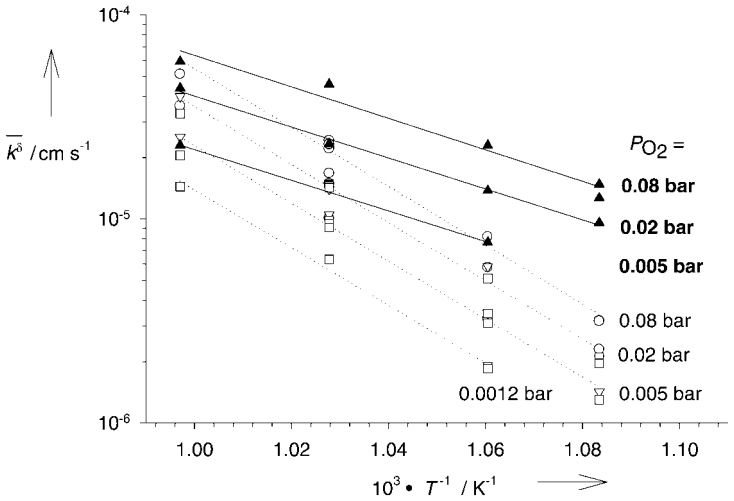

Figure 3. Arrhenius plots of the effective rate constants $\bar{k}^{\delta}$ for oxygen in- (circles) and excorporation (squares) without UV irradiation, and oxygen in- (solid triangles) and excorporation (open triangles) with UV irradiation.

values, while it substantially increased the effective surface rate for jumps to higher P_{O_2} values. The increase in $\bar{k}^{\delta}_{UV}$ was a factor of two at 700 °C and almost a factor of five at 650 °C, and hence leads to a strongly decreased effective activation energy of 145 ± 2 kJ mol^{-1} (Figure 3). Extrapolating to temperatures below 600 °C, we therefore expect more than an order of magnitude difference between $\bar{k}^{\delta}_{UV}$ and $\bar{k}^{\delta}$. The P_{O_2} dependence of $\bar{k}^{\delta}_{UV}$ appears to exhibit no significant difference compared to that for $\bar{k}^{\delta}$ at all the temperatures examined ($\bar{k}^{\delta}_{UV} \propto P_{O_2}{}^{0.37\pm0.10}$); the data at 670 °C is shown in Figure 2b. In Figure 4 it is shown that for jumps to higher oxygen partial pressures, $\bar{k}^{\delta}_{UV}$ displayed an almost linear increase with increasing UV irradiation intensity for two different, final P_{O_2} values at 670 °C. We note that sub-bandgap irradiation at 515 – 700 nm had no effect on the oxygen exchange kinetics.

The possibility that the increase in the relaxation rate is caused by a local temperature increase upon irradiation can be discounted for three reasons: Only the incorporation (and not the excorporation) kinetics were accelerated; sub-bandgap irradiation of similar intensity did not produce an effect; and, in any case, the intensity of the UV radiation is small compared to radiation from the furnace.

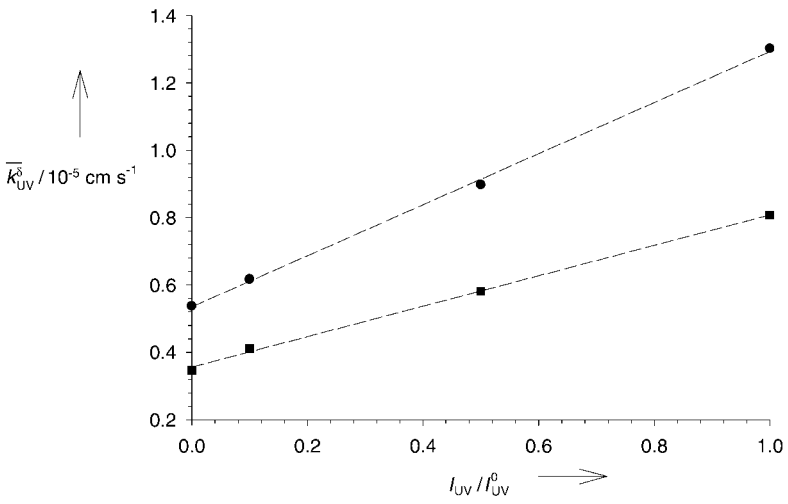

Figure 4. Dependence of $\bar{k}^{\delta}_{UV}$ on UV irradiation intensity at 670 °C for final P_{O_2} values of 0.08 (circles) and 0.02 bar (squares). I^0_{UV} is the full UV intensity; I_{UV} is the intensity attenuated by neutral density filters.

The absorption coefficient α of $SrTiO_3$ for UV radiation is $\sim 10^5$ cm^{-1},[17] from which the photon penetration depth is calculated to be about 100 nm. Unfortunately, there are no literature data on the lifetime of the photogenerated electron – hole pairs in $SrTiO_3$. Values exist for TiO_2 at room temperature and are in the range of 3×10^{-11} to 1×10^{-9} s.[18, 19] Assuming that the values for $SrTiO_3$ are of the same order of magnitude, we estimate the concentration of photogenerated electrons and holes in the irradiated surface layer to be about $3 \times 10^{13} - 1 \times 10^{15}$ cm^{-3}. This is a significant enhancement with respect to the concentration of thermally generated electrons, which is $\sim 2 \times 10^{11}$ cm^{-3}, but negligible compared to the hole concentration of 3×10^{17} cm^{-3} (compare with Figure 1).

The fact that oxygen incorporation is accelerated under UV irradiation, while excorporation remains unchanged, indicates that the sample is far from equilibrium and the UV-accelerated forward reaction rate becomes dominant. Detailed analysis, based on a recent theoretical treatment,[20, 21] of $\bar{k}^{\delta}$ and $\bar{k}^{\delta}_{UV}$ therefore requires knowledge of the exact mechanistic reaction scheme for oxygen incorporation, which is not yet known. Some conclusions can nevertheless be drawn from the experimental data. Since UV irradiation increases, relatively speaking, the electron concentration but not the hole concentration at the surface, this suggests that, for oxygen incorporation, conduction band electrons participate in one or more of the elementary reaction steps up to and including the rate-determining step; quantitative analysis of the relationship between $\bar{k}^{\delta}_{UV}$ and the UV intensity may be expected to provide further mechanistic information in this regard. Since oxygen excorporation is not affected by UV irradiation, this suggests that if any electronic species are involved in surface reaction steps following the rate-determining step, they must be holes.

In short, we have measured the effect of UV irradiation on oxygen incorporation into a model, wide-bandgap electroceramic oxide. The advantage of UV irradiation, in contrast to the other possibilities (changing the temperature, the dopant concentration, or adding catalytic coatings) is that it enables us under isothermal conditions to turn on and off the surface reaction in situ. We will be exploring this effect in the near future with regard to locally structuring electroceramic oxides, and novel optoelectrochemical devices, such as a chemical valve.

Experimental Section

A $SrTiO_3$ single crystal (Frank & Schulte GmbH, Essen, Germany) with an iron content of 4.6×10^{19} cm^{-3} was cut and polished to give a sample with the dimensions $6 \times 6 \times 1$ mm. The large faces exhibited (110) orientation, which upon thermal pretreatment at 900 °C in O_2 became facetted into the more stable (100) and (010) surfaces (indicated by atomic force microscopy).

  1433-7851/01/4011-2128 $ 17.50+.50/0

Oxygen stoichiometry changes were performed between 650 and 730 °C by switching P_{O_2} between $0.0012 \leftrightarrow 0.005 \leftrightarrow 0.02 \leftrightarrow 0.08$ bar (achieved with O_2/Ar mixtures; flow rate 100 mL min^{-1}). The set-up for the in situ optical spectroscopy is described in detail in ref. [15]. The integral Fe^{4+} concentration was monitored continuously by measuring the absorption at 595 nm with a UV/Vis spectrometer (Perkin–Elmer Lambda 2). A narrow bandpass filter was placed between the sample and the detector to block thermal radiation.

For the irradiation experiments, a 200 W Hg high pressure arc lamp (LOT Oriel) was used, whose spectral output was restricted to 280–420 nm by means of UG5 and WG280 filters (Schott). The bandgap of $SrTiO_3$ at 700 °C is 2.7 eV,[15] which corresponds to the absorption of light of 460 nm. The total irradiation intensity was 250 mW cm^{-2} in front of the quartz rod, that acted as light guide to irradiate one of the large faces of the sample, and was attenuated for some experiments by neutral density filters. The UV irradiation was interrupted for ≈30 s at appropriate intervals to permit the 595 nm extinction measurements to be made. The effect of sub-bandgap irradiation of 515–700 nm with a total intensity of 190 mW cm^{-2} was also investigated.

Received: December 27, 2000 [Z16334]

[1] J. Maier, *Angew. Chem.* **1993**, *105*, 558–571; *Angew. Chem. Int. Ed. Engl.* **1993**, *32*, 528–542.
[2] *The CRC Handbook of Solid State Electrochemistry* (Eds.: P. J. Gellings, H. J. M. Bouwmeester), CRC Press, Boca Raton, FL, **1997**.
[3] J. Maier, *Festkörper—Fehler und Funktion. Prinzipien der Physikalischen Festkörperchemie*, Teubner, Stuttgart, **2000**.
[4] *Sensors* (Eds.: W. Göpel, J. Hesse, N. Zemel), VCH, Weinheim, **1987**.
[5] R. Wang, N. Sakai, A. Fujishima, T. Watanabe, K. Hashimoto, *J. Phys. Chem. B* **1999**, *103*, 2188–2194.
[6] G. Munuera, A. R. Gonzalezelipe, J. Soria, J. Sanz, *J. Chem. Soc. Faraday Trans. 1* **1980**, *76*, 1535–1546.
[7] A. Fujishima, K. Honda, *Nature* **1972**, *238*, 37–38.
[8] A. L. Linsebigler, G. Q. Lu, J. T. Yates, *Chem. Rev.* **1995**, *95*, 735–758.
[9] U. Bach, D. Lupo, P. Comte, J. E. Moser, F. Weissörtel, J. Salbeck, H. Spreitzer, M. Grätzel, *Nature* **1998**, *395*, 583–585.
[10] A. Mills, S. Le Hunte, *J. Photochem. Photobiol. A* **1997**, *108*, 1–35.
[11] J. Claus, M. Leonhardt, J. Maier, *J. Phys. Chem. Solids* **2000**, *61*, 1199–1207, and references therein.
[12] R. Waser, *J. Am. Ceram. Soc.* **1991**, *74*, 1934–1940.
[13] G. M. Choi, H. L. Tuller, *J. Am. Ceram. Soc.* **1988**, *71*, 201–205.
[14] N.-H. Chan, R. K. Sharma, D. M. Smyth, *J. Electrochem. Soc.* **1981**, *128*, 1762–1769.
[15] T. Bieger, J. Maier, R. Waser, *Ber. Bunsenges. Phys. Chem.* **1993**, *97*, 1098–1104.
[16] Fitting the measured normalized oxygen-vacancy concentrations with a model including both surface and diffusion contributions yields k^{δ} values which agree (within a relative error of 1%) with the k^{δ} values determined from the exclusively surface-controlled model.
[17] D. Goldschmidt, H. L. Tuller, *Phys. Rev. B* **1987**, *35*, 4360–4364.
[18] G. Rothenberger, J. Moser, M. Grätzel, N. Serpone, D. K. Sharma, *J. Am. Chem. Soc.* **1985**, *107*, 8054–8059.
[19] D. P. Colombo, Jr., R. M. Bowman, *J. Phys. Chem.* **1996**, *100*, 18445–18449.
[20] J. Maier, *Solid State Ionics* **2000**, *135*, 575–588.
[21] J. Maier, *Solid State Ionics* **1998**, *112*, 197–228.

Titanocene-Catalyzed Coupling of Amides in the Presence of Organosilanes To Form Vicinal Diamines**

Kumaravel Selvakumar and John F. Harrod*

Vicinal diamines occur widely in natural products and have many applications in medicinal chemistry and organic synthesis.[1] Despite the existence of many synthetic approaches, there is still a pressing need for better and more general methods based on simple and inexpensive starting materials. We report herein a novel reduction–deoxygenation coupling of amides catalyzed by $[Cp_2TiX_2]$ ($Cp = \eta^5$-cyclopentadienyl; X = Me or F) in the presence of a stoichiometric amount of an organosilane. To the best of our knowledge, such a reaction has not been reported previously, although the literature extensively covers the titanium-mediated coupling of carbonyl[1, 2] and imine[1, 3] compounds in the presence of strong reducing agents.[2] The intramolecular coupling of 1,2-acylamido compounds to form indoles and pyrroles has also been extensively studied.[4]

Both dimethyltitanocene and difluorotitanocene have been used as catalysts for a variety of hydrosilylation reactions.[5–7] We attempted to use these catalysts to effect the hydrosilylation of some amides with $PhMeSiH_2$ and found that the main reaction product in the case of *N*,*N*-dimethylbenzamide was the vicinal diamine, 1,2-dimethylamino-1,2-diphenylethane [Eq. (1)].

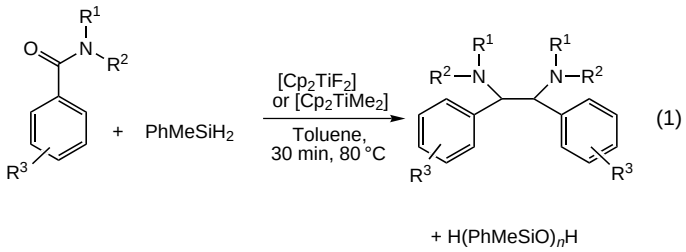

(1)

The effects of a number of chemical and physical variables on the outcome of the reaction are summarized in Tables 1–3. At 80 °C, the reactions of *N*,*N*-dialkylbenzamides and some other related aromatic amides proceed smoothly to give good to excellent yields of the substituted ethylenediamine products (Table 1). Different substituents can be tolerated, as shown in the reactions of 4-chloro-, 4-methoxy-, and 4-trifluoromethylbenzamide. There is no significant difference in the results obtained with the difluoro- and dimethyltitanocene precatalysts. None of the reactions shows significant stereoselectivity.

Reactions at room temperature show an interesting decline in chemoselectivity relative to those carried out at higher temperature (Table 2). Certain substitution patterns also

[*] Prof. Dr. J. F. Harrod, Dr. K. Selvakumar
Department of Chemistry, McGill University
Montreal, QC H3A 2 K6 (Canada)
Fax: (+1) 514-398-3797
E-mail: harrod@chemistry.mcgill.ca

[**] This work was supported by the Natural Sciences and Engineering Research Council (Canada) and the Fonds FCAR du Québec.